Line shifts and broadenings in polarizable liquids

Yong-Cong Chen,[a] Joel L. Lebowitz,[a),b)] and Peter Nielaba[c]
Department of Mathematics, Rutgers University, New Brunswick, New Jersey 08903

(Received 30 December 1988; accepted 21 March 1989)

We present a new dynamical derivation of the approximation used by Thompson, Schweizer, and Chandler and by Høye and Stell for the frequency dependent polarizability of a quantum fluid with harmonically bound dipole moments; the Drude model. The derivation is the same for classical and quantum liquids—as is of course the result which agrees with that of these authors. We then refine the theory by taking account of the limited number of energy levels available, i.e., we replace the harmonic approximation by a two level approximation, for the target atom. This leads to a prefactor ω_{0I}/ω_0 in the line shift of an impurity atom in a fluid computed by Chandler, Schweitzer, and Wolynes: ω_0 and ω_{0I} being the characteristic frequencies of the fluid and impurity atoms, respectively. This factor improves the agreement between theory and experiment, especially those of Nowak and Bernstein on benzene in argon and some other liquids. We also compute the line shapes of the impurity atom by Monte Carlo simulations and obtain reasonable agreement with experimental observations.

I. INTRODUCTION

The evolution of electronic levels as the density of a fluid is changed from that of a very dilute gas to that of a dense liquid is a subject of great intrinsic interest. We have here a situation where by varying the density we can monitor the continuous development of cooperative behavior as we go from an isolated atom to an insulating or metallic liquid, depending on the system and the temperature. Theoretical models for the behavior of such systems require, as a minimum, microscopic treatment of the dielectric response function of a fluid. This is a difficult problem even for the most simplified microscopic models, i.e., fluids consisting of hard sphere atoms each having a fluctuating dipole harmonically bound to its center; the Drude model.

Important steps in the development of a statistical mechanical theory of the static dielectric properties of liquids utilizing techniques such as diagram resummations, integral equations, etc. were taken by Wertheim,[1,2] Høye and Stell,[3] Pratt,[4] and others (see Refs. 1–4). The extension of these ideas to a frequency dependent polarizability was done independently, but essentially identically, by Høye and Stell[5] (HS), and by Thompson, Schweitzer, and Chandler[6] (TSC) and the starting point of their analyses was the extension of classical equilibrium theory techniques to quantum systems. They did this by treating the fluctuating dipole part of the Drude model in the imaginary time formalism of equilibrium quantum mechanics. In that formalism, first derived by Feynman,[7] t is a parameter which varies between zero and $i\beta\hbar$. When the Feynman path is discretized the quantum system looks like a classical liquid of polymers and can be treated accordingly.[8] Application of integral equation methods, such as the mean spherical type approximation, to this polymer fluid, led TSC and HS to an equation for the mean square value of the Fourier transform variable along the path; which is interpretable as the polarizability $\alpha(\omega)$ at imaginary frequencies. Using analytic continuation to real frequencies Chandler, Schweizer, and Wolynes (CSW)[9] then used this $\alpha(\omega)$ to treat the dynamics of line shifts and absorption in pure fluids as well as those containing a dilute solution of impurities. Comparison of theory with experiment[10–12] indicates that the theory does indeed describe certain observed phenomena although it clearly leaves out effects which are central in other cases,[13–15] e.g., it always gives a red shift of the impurity line. The blue shift was discussed semiclassically by Saxton and Deutch[13] and by Messing, Raz, and Jortner[14]; recently it has also been treated in simple quantum schemes by Dobrosavljević, Henebry, and Stratt[16] and by Baer[17]—we shall discuss this in Sec. V.

The interesting part about the CSW analyses is that the final result does not involve $\hbar$ at all. The quantum mechanical (imaginary time) path integral formalism, which was the starting point for making the analogy with classical polymeric fluids (to which the mean spherical approximation is applied), has completely dropped out at the end. This suggests that there ought to be a direct classical way of obtaining the final result. It is in fact what we show here by making an approximation directly on the real time dynamical equations which, for harmonic systems, have the same form classically and quantum mechanically.

We next try to improve on the harmonic approximation in which there are an infinite set of equally spaced energy levels for each atom. While the overall features of the polarization are not expected to be changed by this idealization, provided the occupations of higher levels are small (and this is usually the case for optical transitions), specific predictions of the model about the absorption spectrum may be changed when one takes into account the limited number of internal states involved. To do this we treat the "environment" of an arbitrarily picked (target) atom or impurity as a model harmonic oscillator bath, the so-called boson bath, while taking into account some details of the electronic prop-

[a] Work supported in part by the U. S. Air Force Office of Scientific Research through Grant No. 86-0010.
[b] Also in Department of Physics.
[c] Present address: Institut für Physik, Universität Mainz, Postfach 3980, D-6500 Mainz, West Germany.

 0021-9606/89/130340-10$02.10

erties of the specific atom or impurity. The coupling, which is the usual dipole–dipole interaction, between the target atom and the environment can be determined in this aproximation scheme by first treating the target particle also harmonically in the same way as in HS[5] and TSC.[6] Our model may thus be thought of as a refinement of that theory. We find in fact the same results as in the harmonic approximation for pure fluids but a significant change in the line shift of an impurity immersed in a fluid: the shift obtained by CSW is multiplied by the factor ω_{0I}/ω_0, the ratio of the characteristic frequencies of the solute atom and the solvent fluid. This change is in agreement with the experiments of Nowak and Bernstein.[10–12] Those authors also measured the broadening of the impurity line. This is caused by the fact that different impurity atoms will have different environments and hence there will be a dispersion in the line shifts. We compute the line shape, via Monte Carlo simulations, for the experimental situation considered by Nowak and Bernstein.[10–12] Our results are in qualitative agreement with their findings.

The outline of the rest of the paper is as follows. In the next section we present the new dynamical derivation of the frequency dependent polarizability for the Drude model and consider the line shift and line shape of the impurity absorption spectrum. In Sec. III we investigate in detail the case where the target atom has two levels. In Sec. IV we present the results of Monte Carlo simulations on the impurity line shift and line shape and compare them with experiment. In Sec. V we consider briefly the role of the exchange repulsion and propose a possible scheme to include both the attractive and repulsive interactions. A summary of our results is given in Sec. VI.

II. DERIVATION OF THE DYNAMICAL POLARIZABILITY

We shall derive the TSC and HS result in a real time, classical setting since nothing has to be changed for a harmonic system when going from classical to quantum mechanics—the equations of motion are linear and they also describe the time evolution of the expectation values of the corresponding quantum mechanical operators. We first consider the pure liquid problem; the case of impurities dissolved in the liquid will be considered afterwards. The Hamiltonian for the internal dynamics of an isolated Drude atom (or molecule) is given by

$$H_0=\frac{\mathbf{P}^2}{2M}+\frac{1}{2}M\omega_0^2\mathbf{Q}^2,\quad M=\frac{1}{\alpha_0\omega_0^2}, \tag{2.1}$$

where α_0 and ω_0 are, respectively, the static polarizability and the characteristic frequency of the atom; $\mathbf{Q}=(Q_x,Q_y,Q_z)$ is the three dimensional dipole moment and $\mathbf{P}$ the conjugate momentum. The total interaction potential for an N particle system can be written as

$$U(1,2,...,N)=\sum_{i<j\leqslant N}u(i,j), \tag{2.2}$$

where i stands for both $\mathbf{r}_i$, the position of the center of the ith atom and $\mathbf{Q}_i$ its internal coordinate. $u(i,j)$ consists of a spherically symmetric reference potential, usually assumed to be a hard-core repulsion and a dipole–dipole interaction, i.e.,

$$u(i,j)=u_0(r_i,r_j)-\mathbf{Q}_i\cdot\mathbf{T}(\mathbf{r}_i-\mathbf{r}_i)\cdot\mathbf{Q}_j, \tag{2.3}$$

with the tensor $\mathbf{T}$ given by

$$\mathbf{T}(\mathbf{r})=(3\mathbf{rr}/r^2-\mathbf{I})/r^3. \tag{2.4}$$

We now make the essential assumption that, in response to a high-frequency field only the internal degrees of freedom, i.e., the polarizations, follow the field while the $\{\mathbf{r}_i\}$ can be considered stationary during the course of photon absorption.[18] The justification for this assumption is that the motion of the positions of the atoms is usually very slow compared to the time scale of the internal motion. Thus the only thing we need to do about the $\{\mathbf{r}_i\}$ is to average over their distribution.[5,6] Once this is accepted the (approximate) time dependent linear polarizability can be derived in exactly the same way as that used by Wertheim[1] and Pratt[4] for the static, $\omega=0$, case. We shall therefore only sketch the derivation referring to those authors for details.

Given a configuration of the positions of the atoms, we can readily write down the equations of motion for the average polarizations $\bar{\mathbf{Q}}_i(t)$ (given fixed $\{\mathbf{r}_j\}$) in response to a spatially uniform external oscillating electric field $\mathbf{E}(\omega)\times\exp(-i\omega t)$. The average here is with respect to some initial distribution of the $\mathbf{Q}$'s at time t_0 with $t_0\to-\infty$. The Fourier transform of the equation is

$$\alpha_0^{-1}(\omega)\bar{\mathbf{Q}}_i(\omega)-\sum_{j=1,\neq i}^{N}\mathbf{T}(\mathbf{r}_i-\mathbf{r}_j)\cdot\bar{\mathbf{Q}}_j(\omega)=\mathbf{E}(\omega), \tag{2.5}$$

where $\alpha_0(\omega)$ is the isolated atom polarizability,

$$\alpha_0(\omega)=\frac{\alpha_0}{1-(\omega/\omega_0)^2}. \tag{2.6}$$

It is convenient to introduce the $N\times N$ matrix

$$\mathbf{M}_{ij}=\alpha_0(\omega)\mathbf{T}(\mathbf{r}_i-\mathbf{r}_j)(1-\delta_{ij}). \tag{2.7}$$

We can then write down formally a steady state solution of Eq. (5)

$$\begin{aligned}\bar{\mathbf{Q}}_i(\omega)&=\sum_j(\mathbf{I}\delta_{ij}-\mathbf{M}_{ij})^{-1}\alpha_0(\omega)\mathbf{E}(\omega)\\&=\sum_{j=1}^{N}\sum_{n=0}^{\infty}(M^n)_{ij}\alpha_0(\omega)\mathbf{E}(\omega).\end{aligned} \tag{2.8}$$

We should now average Eq. (2.8) over the approximate ensemble distribution of the $\{\mathbf{r}_i\}$, the positions of the atoms. Since we are interested only in linear terms in the field we can use the distribution obtained from the Gibbs measure in the absence of a field, i.e., the measure obtained from $\exp\{-\beta[\Sigma H_0(i)+\Sigma u_{ij}]\}$ after integrating out the Q's. Denoting this average by $\langle\cdots\rangle$ $\langle\mathbf{Q}_1(\omega)\rangle$ can be written as

$$\begin{aligned}\langle\mathbf{Q}_1(\omega)\rangle&=\sum_{n=0}^{\infty}\sum_{j_1}\cdots\sum_{j_n}C(j_1,j_2,\cdots,j_n)\cdot\mathbf{E}(\omega)\\&\equiv\alpha(\omega)\mathbf{E}(\omega),\end{aligned} \tag{2.9}$$

where

$$\begin{aligned}C_n(j_1,j_2,\cdots,j_n)=[\alpha_0(\omega)]^n\langle&\mathbf{T}(\mathbf{r}_1-\mathbf{r}_{j_1})\\&\cdot\mathbf{T}(\mathbf{r}_{j2}-\mathbf{r}_{j3})\cdots\mathbf{T}(\mathbf{r}_{jn-1}-\mathbf{r}_{j_n})\rangle.\end{aligned} \tag{2.10}$$

Note that ω enters explictly in Eq. (2.9) only through $\alpha_0(\omega)$. Hence the resulting frequency dependent linear polarizability $\alpha(\omega)$ will have the same dependence on $\alpha_0(\omega)$ as the static $\alpha(0)$ has on $\alpha_0(0)=\alpha_0$. To indicate the type of approximation required to get the result of,[5,6] it is convenient to represent Eq. (2.10) in terms of diagrams, see Refs. 1 and 2. Note that terms in which an index j_k occurs an odd number of times will vanish after the average over $\{\mathbf{r}_i\}$. As a result, we must have $j_n=1$ which means that the fields acting on the other particles do not contribute to $\langle \mathbf{Q}_1(\omega)\rangle$. The remaining chains, starting and ending at atom 1, include loops closing at an arbitrary atom. Using now the type of approximation discussed by Wertheim,[1] where only "simple self-closing" (SSC) graphs are permitted and making a superposition approximation at vertices with more than two bonds, the "dangling" loops can be conveniently included into the "self-energy" of that atom, i.e., we replace the bare atomic polarizability $\alpha_0(\omega)$ by $\alpha(\omega)$, the effective atomic polarizability to be calculated. This yields a self consistency equation for the frequency dependent polarizability, cf. Eq. (3.7) in Pratt,[4]

$$\frac{1}{\alpha(\omega)}=\frac{1}{\alpha_0(\omega)}-2\mathscr{E}[\alpha(\omega)], \tag{2.11}$$

where we have introduced, as in Refs. 4–6 the function $\mathscr{E}[\alpha(\omega)]$

$$\mathscr{E}(\alpha)=\frac{1}{2}\left\langle \sum_{n=1}^{\infty}\left(\sum_{j_1,\cdots j_n}\alpha^n \hat{\mathbf{E}}\cdot\mathbf{T}(\mathbf{r}_1-\mathbf{r}_{j_1})\cdot\mathbf{T}(\mathbf{r}_{j_1}-\mathbf{r}_{j_2})\right.\right.$$
$$\left.\left.\times\cdots\mathbf{T}(\mathbf{r}_{jn}-\mathbf{r}_1)\cdot\hat{\mathbf{E}}\right)\right\rangle \tag{2.12}$$

with $\hat{\mathbf{E}}$ being the unit vector in the direction of $\mathbf{E}$ and the sum restricted to the diagrams in which all the j_i's are different.

Following Pratt, TSC, and HS, it is useful to think of the right-hand side of Eq. (2.10) as an average over a dipolar liquid where each atom has a permanent dipole $\mathbf{d}$. Denoting the average over the angle of the dipole by $\int d\Omega/4\pi$ and noting that

$$\mathbf{T}(\mathbf{r}_1-\mathbf{r}_3)\cdot\mathbf{T}(\mathbf{r}_3-\mathbf{r}_2)$$
$$=\frac{3}{|\mathbf{d}|^2}\int\frac{d\Omega_3}{4\pi}\mathbf{T}(\mathbf{r}_1-\mathbf{r}_3)\cdot\hat{\mathbf{d}}_3\,\hat{\mathbf{d}}_3\cdot\mathbf{T}(\mathbf{r}_3-\mathbf{r}_2), \tag{2.13}$$

we can rewrite Eq. (2.12), see Eq. (3.6) in Pratt,

$$\mathscr{E}(\alpha)=\frac{1}{2}\frac{\rho}{(4\pi)^2V}\int d\,1\,d\,2\,\hat{\mathbf{d}}_1\cdot\mathbf{T}(12)\cdot\hat{\mathbf{d}}_2\,G(21,\alpha), \tag{2.14}$$

where $dj=d\mathbf{r}_j\,\Omega_j$, V is the volume and $\rho=N/V$ the number density of atoms. The quantity $G(21,\alpha)$ is formally the same as the deviation of the two particle distribution function of the dipolar liquid from its value in the reference system with potential $u_0(\mathbf{r}_i,\mathbf{r}_j)$ in the mean spherical approximation if we set $|\mathbf{d}|^2=3kT\alpha$:

$$G(12,\alpha)=(3\alpha)\mathbf{d}_2\left\{\mathbf{T}(21)g(12)\right.$$
$$+\left(\frac{3\alpha\rho}{4\pi}\right)\int d\,3\,g(123)\mathbf{T}(23)\cdot\mathbf{d}_3\,\mathbf{d}_3\cdot\mathbf{T}(31)$$
$$+\left(\frac{3\alpha\rho}{4\pi}\right)^2\int d\,3d\,4\,g(1234)\mathbf{T}(23)\cdot\mathbf{d}_3\mathbf{d}_3$$
$$\left.\cdot\mathbf{T}(34)\cdot\mathbf{d}_4\,\mathbf{d}_4\cdot\mathbf{T}(41)+\cdots\right\}\cdot\mathbf{d}_1, \tag{2.15}$$

where $g(12\cdots k)$ is the k particle distribution function.

There are many useful approximations in the literature for the pair distribution function $G(21,\alpha)$. For a relevant review we refer readers to the work by Rushbrooke *et al.*[19] where several approximation schemes are compared: a simple approximation is to use the exact expression[20] for $G(12,\alpha)$ at low density with

$$g_0(12\cdots k)=\prod_{i<j\leqslant k}\exp\left[-\frac{u_0(\mathbf{r}_i,\mathbf{r}_j)}{kT}\right].$$

A better approximation, appropriate at higher density, can be obtained by using a Padé construction[19] based on more precise considerations of the first few coefficients of Eq. (2.15). This approximation was used by CSW[9] to solve the self-consistency equation. (There is a typographic error in Ref. 9 concerning the integrals I_2 and I_3 [related to the first two coefficients in Eq. (2.15)]. The two quantities should be as given in Pratt's paper[4] rather than those appearing in Ref. 19. The two sources (Refs. 4 and 19) have slightly different definitions of the integrals up to some constant factors.)

Whatever approximation is used for $\alpha(\omega)$, it is necessary to use[9] $\omega\to\omega+i0^+$ to find the imaginary part of the polarizability which turns out to be nonzero in a certain regime. This can be understood by considering the picture of adiabatically switching on the external field. The presence of the imaginary part is an indication of energy absorption by the liquid from the external field and is normally associated with the density of the excited states.[9] It is found that even if we keep only the first term on the right-hand side of Eq. (2.12), the excitation spectrum has a finite bandwith corresponding to nonzero Im $\alpha(\omega)$.

A. Impurity polarizability

Let us now consider the case where atom 1 is a solute atom with static polarizability α_{0I} and characteristic frequency ω_{0I}. We then simply replace the matrix elements in Eq. (2.7) by

$$\mathbf{M}_{1j}\to\alpha_{0I}(\omega)\mathbf{T}(\mathbf{r}_1-\mathbf{r}_j) \tag{2.16}$$

with atom 1 being the impurity atom and

$$\alpha_{0I}(\omega)=\frac{\alpha_{0I}}{1-(\omega/\omega_{0I})^2}. \tag{2.17}$$

Similarly in considering the self-closing loops at atom 1 $\alpha_0(\omega)$ is replaced by $\alpha_{0I}(\omega)$. We then have, following the same considerations as above, the equation for the impurity polarizability

$$\frac{1}{\alpha_I(\omega)}=\frac{1}{\alpha_{0I}(\omega)}-2\tilde{\mathscr{E}}[\alpha(\omega)]. \tag{2.18}$$

In Eq. (2.18) $\alpha(\omega)$ should be determined from the pure liquid Eq. (2.11) and $\tilde{\mathscr{E}}(\alpha)$ may differ from $\mathscr{E}(\alpha)$ if the solute atom has a different radius. In fact, we should now use everywhere in Eq. (2.12) the corresponding two-component distribution functions with the impurity atom being the second component. This somewhat complicates the computation. Fortunately, in practice one often needs to evaluate only the two-particle term; the higher order terms are usually negligible in magnitude [this is however not the case for the pure liquid because $\alpha(\omega)$ can be divergently large in the vicinity of ω_0].

B. Impurity absorption spectrum

We can obtain an effective ω_I by setting the right side of Eq. (2.18) equal to zero. This ω_I is shifted relative to ω_{0I} by

$$\omega_I - \omega_{0I} \simeq -\alpha_{0I}\omega_{0I}\tilde{\mathscr{E}}[\alpha(\omega_{0I})], \tag{2.19}$$

which is a red shift (whenever the bare impurity frequency $\omega_{0I} < \omega_0$). It is also possible to consider the distribution of ω_I by noting that the effective impurity polarizability is not obtained through any self-consistency consideration. In fact, we can consider the polarization of a particular impurity atom before taking the ensemble average over the positions of the surrounding solvent atoms. In this case, Eq. (2.18) still holds approximately (ignoring the effects coming from the external fields acting on the other atoms) and the quantity $\tilde{\mathscr{E}}[\alpha(\omega)]$ entering there is now a fluctuating variable depending on the distribution of the surrounding atoms. There might be some questions with regard to replacing $\alpha_0(\omega)$ by $\alpha(\omega)$ for the solvent atoms before taking the ensemble average. We could, however, also use the exact expression (2.10) as a starting point.

Given a configuration of the solvent atoms, we can in principle compute a corresponding new absorption frequency of that impurity. But there are many individual impurities! Hence, rather than regarding the absorption band of the impurity as being a δ function,[9] one has the following expression for the intensity of the impurity spectrum,

$$I(\omega) \propto \langle \boldsymbol{\delta}[\omega - \omega_I(\{\mathbf{r}_2,\ldots,\mathbf{r}_N\})]\rangle, \tag{2.20}$$

with

$$\omega_I(\{\mathbf{r}_2,\ldots,\mathbf{r}_N\}) = \omega_{0I}[1 - \alpha_{0I}\tilde{\mathscr{E}}[\alpha(\omega_{0I})]], \tag{2.21}$$

where $\tilde{\mathscr{E}}[\alpha(\omega_{0I})]$ is given by Eq. (2.12). Alternatively, one can replace $\alpha(\omega)$ by $\alpha_0(\omega)$ in Eq. (2.12) and allow repeated summations over the intermediate atoms. The latter scheme is useful in the computer simulations.

The calculation of the line shape is highly nontrivial since one has to know essentially the total N particle ensemble distribution (rather than just few-particle correlation functions); analytical techniques, at the present, are not readily available. On the other hand, computer simulations seem to be rather efficient. For illustration we present here a simple analytic calculation of the second moment; Monte Carlo simulations will be discussed in Sec. IV.

C. The second moment of the impurity spectrum

To simplify the calculation let us keep only the leading term in $\tilde{\mathscr{E}}(\alpha)$,

$$\tilde{\mathscr{E}}(\alpha) = \frac{\alpha}{2}\sum_{N\geq j>1} \hat{\mathbf{E}}\cdot\mathbf{T}^2(1j)\cdot\hat{\mathbf{E}} + O(\alpha^2). \tag{2.22}$$

We shall assume that both the solute and solvent consist of hard core atoms with R the solvent–solvent and $\tilde{R}$ the solvent–solute hard core exclusion diameters. Using the low-density limit of the distribution functions $g(12)$ and $g(123)$ [see discussion following Eq. (2.15)], we find that

$$\langle \tilde{\mathscr{E}}(\alpha)\rangle = \frac{4\pi}{3\tilde{R}^3}\alpha\rho, \tag{2.23}$$

and the second moment of the distribution is

$$\langle [\tilde{\mathscr{E}}(\alpha)]^2\rangle - [\langle \tilde{\mathscr{E}}(\alpha)\rangle]^2 = A\rho\alpha^2 - B\rho^2\alpha^2, \tag{2.24}$$

with

$$A = \frac{8\pi}{15\tilde{R}^9} \tag{2.25}$$

and

$$B = 4\pi^2\int_{\tilde{R}}^{\infty}\frac{dr}{r^4}\int_{R}^{\infty}\frac{dr'}{r'^4}\{2 - \tfrac{9}{5}f(r,r') - \tfrac{1}{5}[f(r,r')]^3\}\times\theta(R - |r - r'|), \tag{2.26}$$

where $\theta(x)$ is the step function and

$$f(r,r') = \frac{r^2 + r'^2 - R^2}{2rr'}. \tag{2.27}$$

The quantity B can be computed either analytically or numerically. In the low-density regime the second term on the right-hand side of Eq. (2.24) is usually small. Hence the variance is scaled roughly as $\sqrt{\rho}$. This feature should be observable in experiment. Note, however, that it may differ from the half width usually measured in experiment; the latter $\propto\rho$ at low densities, see Fig. 3 in Sec. IV.

III. A TARGET-ENVIRONMENT CONSIDERATION

A. The environment of a target atom

The system we have considered so far can be thought of as special cases of a target atom coupled to an environment in which all terms in the Hamiltonian are quadratic in the **Q**'s. We now wish to analyze situations where the isolated target atom need not be treated as a harmonic oscillator while still representing the environment as an idealized bath of oscillators (normal modes) with linear couplings to the target atom. More precisely, we consider the following total effective Hamiltonian

$$H = \tilde{H}_0 + \sum_k\left(\mathbf{Q}\cdot\mathbf{C}_k x_k + \frac{p_k^2}{2m_k} + \frac{1}{2}m_k\omega_k x_k^2\right), \tag{3.1}$$

where $\tilde{H}_0$ is the bare Hamiltonian of the target atom. The parameters entering H can be determined from the harmonic approximation by replacing $\tilde{H}_0$ by H_0 given in Eq. (2.1), when the target particle is a solvent atom (the case of an impurity target atom will again be considered later). We shall further assume that motions in different directions are decoupled, i.e., if we apply an external electric field $\mathbf{E}(t)$ in the z direction, only the motion of Q_z will be affected. This can be imposed for example by assuming that $\mathbf{C}_k$ has only one nonvanishing component in the z direction. While this is not true in general the situation in an isotropic liquid is likely to be such that the different components of C_k are randomly distributed so that the average effect of the coupling vanishes. To avoid unnecessary complications we shall simply drop the vector notation in the above equations.

The Fourier transform of the equation of motion (in the z direction) when $\tilde{H}_0 = H_0$ can now be readily written down

$$\alpha_0(\omega)Q_1(\omega) + \sum_k C_k x_k(\omega) = E(\omega), \tag{3.2}$$

$$-m_k\omega^2 x_k(\omega) + m_k\omega_k^2 x_k(\omega) + C_k Q(\omega) = E_k(\omega), \tag{3.3}$$

where $E_k(\omega)$ represents the effective driving force on the k th mode. Note that the average of the driving forces $\{E_k\}$, taken with respect to the ensemble distribution of the environmental atoms, should vanish. We shall hereafter ignore them. Introducing the following "spectrum of coupling"

$$J(\omega) = \frac{\pi}{2}\sum_k \frac{C_k^2}{m_k\omega_k}\delta(\omega-\omega_k), \tag{3.4}$$

we then obtain, in the limit when the spectrum becomes continuous,

$$\frac{2}{\pi}\int d\omega' \frac{J(\omega')\omega'}{(\omega+i0^+)^2-\omega'^2} = \frac{1}{\alpha_h(\omega)} - \frac{1}{\alpha_0(\omega)}, \tag{3.5}$$

where $\alpha_h(\omega)$ stands for the pure harmonic polarizability which is determined through Eq. (2.11). This leads immediately to the relation

$$J(\omega) = \frac{\alpha_h''(\omega)}{\alpha_h'^2(\omega)+\alpha_h''^2(\omega)}, \quad \alpha_h(\omega) = \alpha_h'(\omega) + i\alpha_h''(\omega). \tag{3.6}$$

For an impurity target we should replace $\alpha_0(\omega)$ by $\alpha_{0I}(\omega)$ in Eq. (3.5) and determine $\alpha_h(\omega)$ through Eq. (2.18), where $\tilde{\mathscr{E}}(\alpha)$ is used.

B. The polarizability of a two-level target

We now consider a specific model for the target atom or impurity. Suppose that the groundstate of the atom is an S state and the excited states are the three polarization states $|x\rangle$, $|y\rangle$, and $|z\rangle$ with angular momentum number $l=1$. Again, if the external field is applied in the z direction, only the excited state $|z\rangle$ will be involved, since by assumption different directions are not coupled.

It is convenient to write the total Hamiltonian (3.1) in the following form

$$H = \frac{\hbar\Omega_0}{2}\sigma_z + \sum_k [D\tilde{C}_k(\sigma_+ + \sigma_-)(\alpha_k^\dagger + \alpha_k) + \hbar\omega_k\alpha_k^\dagger\alpha_k], \tag{3.7}$$

where σ's are the Pauli spin matrices,

$$\tilde{C}_k = \sqrt{\hbar/2m_k\omega_k}\,C_k, \tag{3.8}$$

and $D=\langle S|Q_z|z\rangle$ is the dipole matrix element. This is a standard spin-boson Hamiltonian. We will consider only the weak coupling case, since in practice the effect of the environment in our problem is usually small. Note that if we consider the impurity problem, then Ω_0 becomes the frequency of the impurity which differs from ω_0.

It is easy to find, to first order in the coupling, the new ground-state wave function

$$|\Psi_0\rangle = N_0\left[1 - D\sum_k \frac{\tilde{C}_k a_k^\dagger\sigma_+}{\hbar(\Omega_0+\omega_k)}\right]|\Phi_0\rangle, \tag{3.9}$$

where $|\Phi_0\rangle$ is the unperturbed ground state and N_0 is the normalization factor. The new ground-state energy is

$$\tilde{E}_0 = -\left(\frac{\hbar\Omega_0}{2}+\delta E_0\right), \tag{3.10}$$

where δE_0 is the second-order correction to the old groundstate energy

$$\delta E_0 = D^2\int \frac{d\omega\, J(\omega)}{\pi(\Omega_0+\omega)}. \tag{3.11}$$

Note that all three directions of the polarization contribute equally to the new ground-state energy. Therefore, the actual correction to the groundstate energy is three times δE_0. However, in our two-state truncation we shall ignore all the influences from other directions since they simply add a constant shift to all the energies.

It is slighly complicated to find the modified low level excited states—they are *quasicontinuous*. We shall take a two-step approach: (1) Find the exact eigenstates in the rotating wave approximation[21] so that all the eigenstates near a given energy are properly treated; (2) find the first corrections of the remaining perturbation to the energy shift between the ground and excited states.

In the rotating wave approximation the terms $\alpha_k^\dagger\sigma_+$ and $a_k\sigma_-$ in Eq. (3.7) are ignored (due to, presumably, the mismatch of the rotating quantum mechanical phases). The eigenstates can then be found exactly[21]

$$|\Phi_1(q)\rangle = N_1(q)\left[\sigma_+ + \sum_k \frac{D\tilde{C}_k a_k^\dagger}{\hbar(q-\omega_k+\Omega_0)}\right]|\Phi_0\rangle, \tag{3.12}$$

where

$$N_1(q) = \left[1 + \sum_k \frac{\tilde{C}_k^2 D^2}{\hbar^2(q-\omega_k+\Omega_0)^2}\right]^{-1/2} \tag{3.13}$$

is a normalization constant and the parameter q satisfies the equation

$$\hbar q - \sum_k \frac{\tilde{C}_k^2 D^2}{\hbar(q-\omega_k+\Omega_0)} = 0. \tag{3.14}$$

The corresponding energy spectrum is (ignoring zero point oscillations of the bath)

$$E_1(q) = \hbar q + \frac{\hbar\Omega_0}{2}. \tag{3.15}$$

We are of course interested in the limit where the bath degrees of freedom become infinite. Equations (3.12)–(3.15) are not yet suited for taking this limit. The equation determining q involves all the states of the bath; whereas the normalization $N_1(q)$ is a "local quantity" since it has a denominator proportional to $(q-\omega_k+\Omega_0)^2$, indicating that states far away from $q-\omega_k+\Omega_0\cong 0$ are unimportant (their contributions are $\propto \rho^{-2}$ where ρ is the density of states of the bath, see below). Notice that there is always a solution of Eq. (3.14), $q=q_k$, with $\omega_k-\Omega_0<q_k<\omega_{k+1}-\Omega_0$; the precise location of q_k is important for $N_1(q_k)$. Moreover, if $\omega_k-\Omega_0\neq 0$ for all ω_k's, there is an "isolated mode" near $q=0$, which induces a small shift in the unperturbed excited energy $\hbar\Omega_0/2$.

It is of central importance to determine the normalization constant $N_1(q)$ in the continuum limit. A straightforward determination usually requires certain assumptions on the smoothness of the coupling and energy spectrum which should however not affect the final result. In fact, it is possible to take the limit in a more elegant way, see Ref. 22 (which, nevertheless, still involves certain sensitive changes of limits). In this paper, we shall do it in an intuitive way which, we believe, is more helpful for understanding the underlying physics. Let us divide, for a given q_k, the sum Σ_k into two parts; corresponding to "remote" and "local" contributions. The remote ones can be readily treated in terms of a principal integral over the frequency, while the local ones have to be treated in a discretized manner. Assuming that in the vicinity of q_k both the frequency spectrum and the coupling coefficients are uniform, Eq. (3.14) yields

$$\hbar q_k - \int \frac{d\omega}{\pi} \mathscr{P} \frac{D^2 J(\omega)}{(q_k - \omega + \Omega_0)} - \frac{D^2 \tilde{C}_k^2 \rho(\omega_k)}{\hbar} \sum_n \frac{1}{\rho(\omega_k)\delta q_k - n} = 0, \tag{3.16}$$

with

$$\delta q_k = q_k - \omega_k + \Omega_0 \tag{3.17}$$

and $\rho(\omega_k)$ being the local density of frequencies. Note that the local summation is proportional to $\text{cotan}[\pi\rho(\omega_k)\delta q_k]$ if we let n range over all integers [which corresponds to $\rho(\omega_k) \to \infty$]. We thus obtain, ignoring the subscript k,

$$\delta q = \frac{1}{\pi\rho(q+\Omega_0)} \arctan\left[\frac{D^2 J(q+\Omega_0)}{\hbar\tilde{q}}\right], \tag{3.18}$$

where

$$\tilde{q} = q - \int \frac{d\omega}{\pi} \mathscr{P} \frac{D^2 J(\omega)}{\hbar(q - \omega + \Omega_0)}. \tag{3.19}$$

Using this result, it is not difficult to find the normalization factor $N_1(q)$. For the isolated mode $N_1(q) \simeq 1$, whereas for the continuous modes, we have [cf. Eqs. (3.13), (3.14), and the discussion following Eq. (3.15)]

$$N_1(q) = \left(1 + \frac{D^2 J(q+\Omega_0)}{\hbar} \frac{\partial}{\partial \delta q} \text{cotan}[\pi\rho(q+\Omega_0)\delta q]\right)^{-1/2} \simeq \left(\frac{D^2 J(q+\Omega_0)/\hbar}{\pi\rho(q+\Omega_0)\{\tilde{q}^2 + [D^2 J(q+\Omega_0)/\hbar]^2\}}\right)^{1/2}. \tag{3.20}$$

To carry out the second step mentioned earlier, we now calculate, using $|\Phi_1(q)\rangle$ as the basis, the contribution of $a_k\sigma_-$ and $a_k^\dagger\sigma_+$. This is a simple second order perturbation calculation. Note that the only kind of states that have matrix elements connected to $|\Psi_1(q)\rangle$ are $\sigma_+ a_k^\dagger a_{k'}^\dagger |\Phi_0\rangle$. These states, not contributing to the matrix element inducing the polarization [see Eq. (3.28)], may appreciately modify the excited state energy. To second order of the perturbation, we have

$$\tilde{E}_1(q) = \hbar q + \frac{\hbar\Omega_0}{2} - \delta E_1(q), \tag{3.21}$$

where

$$\delta E_1(q) = N_1^2 \sum_{k,k'} \left| \langle\Phi_0| a_k a_{k'} \left[\sum_l D\tilde{C}_l a_l^\dagger\right]\left[\sum_{l'} \frac{D\tilde{C}_{l'} a_{l'}^\dagger}{\hbar(q - \omega_{l'} + \Omega_0)}\right] |\Phi_0\rangle \right|^2 [2\hbar(\omega_k + \omega_{k'} - q)]^{-1}$$
$$= N_1(q)^2 \sum_{k,k'} \frac{D^2\tilde{C}_k^2}{\hbar(\omega_k + \omega_{k'} - q)} \frac{D^2\tilde{C}_{k'}^2}{\hbar^2(q - \omega_{k'} + \Omega_0)^2}. \tag{3.22}$$

For the continuous modes,

$$\delta E_1(q) \simeq \sum_k \frac{D^2\tilde{C}_k^2}{\hbar(\omega_k + \Omega_0)} = \delta E_0 \tag{3.23}$$

which indicates that the relative energy between the ground and excited states is not changed. However, for the isolated mode, $\delta E_1(q)$ is some higher order quantity compared to δE_0.

We can now apply an external oscillating field to the atom. The extra time-dependent Hamiltonian can be written as

$$H'(t) = E(t)D(\sigma_+ + \sigma_-), \tag{3.24}$$

where $E(t)$ can be further written as

$$E(t) = \int d\omega\, E(\omega)\exp[-i(\omega + i0^+)t]. \tag{3.25}$$

Let us decompose the total time-dependent wave function into

$$|\Psi(t)\rangle = A_0(t)\exp[-iE_0 t/\hbar]|\Psi_0\rangle + A_1(q,t)\exp[-iE_1(q)t/\hbar]|\Psi_1(q)\rangle, \tag{3.26}$$

where E_0 and $E_1(q)$ are given, respectively, by Eqs. (3.10) and (3.11). It is straightforward to find, in the linear response approximation, the frequency dependent polarizability

$$\alpha(\omega) = \sum_q \frac{2D^2(E_1(q) - E_0)|\langle\Psi_0|(\sigma_+ + \sigma_-)|\Psi_1(q)\rangle|^2}{\hbar[(E_1(q) - E_0)^2/\hbar^2 - (\omega + i0^+)^2]}. \tag{3.27}$$

The matrix elements in Eq. (3.27) can be evaluated explicitly,

$$\langle\Psi_0|(\sigma_+ + \sigma_-)|\Psi_1(q)\rangle = N_0 N_1(q)\left[1 - \sum_k \frac{D^2\tilde{C}_k^2}{\hbar^2(\Omega_0 + \omega_k)(q - \omega_k + \Omega_0)}\right] \cong N_1(q)\left[1 - \frac{q}{q + 2\Omega_0}\right]. \tag{3.28}$$

These results are rather independent of the detailed structure of the spectrum and thus can be applied to quite general situations. In particular, we do not have to restrict ourselves to the case where the absorption bandwidth of the liquid is small. We shall discuss below the resulting impurity and pure liquid polarizations.

C. The impurity frequency shift

In this case, $\Omega_0 = \omega_{0I}$ is the impurity frequency and the spectrum consists of an isolated mode near $q = 0$ (namely the unperturbed excited energy) and a continuous part coinciding with the solvent's own spectrum. Since the changes in the continuous spectrum induced by the impurity are very weak, they are usually unobservable. For the isolated mode, the central question is the frequency shift due to the presence of the coupling to the solvent. The new resonance frequency is located where the denominator of the right-hand side of Eq. (3.27) becomes zero,

$$\omega_I = \omega_{0I} + \frac{\delta E_0}{\hbar} + \int \frac{d\omega}{\pi} \frac{D^2 J(\omega)}{\hbar(\omega_{0I} - \omega)}$$

$$\cong \omega_{0I} + \frac{\alpha_{0I}\omega_{0I}^2}{2\omega_0}\left[\frac{1}{\alpha_h(\omega_{0I})} - \frac{1}{\alpha_0(\omega_{0I})}\right], \qquad (3.29)$$

where in the second equality we have implicitly assumed that the absorption bandwidth is small compared to ω_{0I} and centered near it. In Eq. (3.29),

$$\alpha_{0I} \equiv \frac{2D^2}{\hbar\omega_{0I}} \qquad (3.30)$$

is the unperturbed static polarization of the impurity. Furthermore, using the self-consistency equation (2.18) we can rewrite the frequency shift as

$$\omega_I - \omega_{0I} = -\left(\frac{\omega_{0I}}{\omega_0}\right) \times \alpha_{0I}\omega_{0I}\tilde{\mathscr{E}}\left[\alpha_h(\omega_{0I})\right] \qquad (3.31)$$

which corresponds to the result of Chandler, Schweizer, and Wolynes[9] *multiplied* by a factor ω_{0I}/ω_0. This extra factor greatly improves the agreement in absolute magnitude between theory and experiment for the benzene ${}^1B_{2u} \rightarrow {}^1A_{1g}$ transition in argon liquid and some other solvents[10–12] see Fig. 3 and Table I in the next section.

D. The pure liquid polarizability

For the pure liquid case, $\Omega_0 = \omega_0$, and there are no isolated modes and no overall relative frequency shift between the ground-state and the excited states. After some manipulations, Eq. (3.27) yields the resulting polarizability

$$\alpha(\omega) = \frac{2}{\pi}\int d\omega' \frac{\tilde{J}(\omega')\omega'}{\omega'^2 - (\omega + i0^+)^2} \qquad (3.32)$$

$$\tilde{J}(\omega) = \frac{\alpha_0^2 J(\omega)/4}{(\alpha_0 J(\omega)/2)^2 + [\omega - \tilde{\omega}_0(\omega)]^2/\omega_0^2}, \qquad (3.33)$$

where

$$\tilde{\omega}_0(\omega) = \omega_0 - \int \frac{d\omega'}{\pi}\mathscr{P}\frac{D^2 J(\omega')}{\hbar(\omega' - \omega)}, \quad \alpha_0 = \frac{2D^2}{\hbar\omega_0}. \qquad (3.34)$$

In the *small bandwidth limit*, we can further rewrite

$$\tilde{\omega}_0(\omega) \cong \omega_0\left\{1 + \frac{\alpha_0}{2}\mathrm{Re}\left[\frac{1}{\alpha_h(\omega)} - \frac{1}{\alpha_0(\omega)}\right]\right\}$$

$$\cong \omega + \mathrm{Re}\frac{\alpha_0}{2\alpha_h(\omega)}. \qquad (3.35)$$

This gives, after some algebra, not too surprisingly

$$\tilde{J}(\omega) = \alpha_h''(\omega). \qquad (3.36)$$

This shows explicitly that *in the small bandwidth limit our spin-boson model does not change the pure liquid polarization obtained from the harmonic oscillator approximation by* HS[5] *and* TSC.[6]

IV. COMPUTER SIMULATIONS AND COMPARISON WITH EXPERIMENT

As mentioned earlier analytical calculations on the line shapes of the impurity spectrum require essentially the complete ensemble distribution of the solvent atoms. We therefore turn to Monte Carlo simulations.[23,24] For simplicity we assume that both the solvent and solute atoms are hard spheres with their own hard-core diameters. To carry out the simulations we have taken a system with 124 solvent particles in an adjustable (periodic) box so that the reduced density can be varied. The impurity was fixed (at the center of the box) while the positions of the solvent particles were randomly distributed. At a given solvent configuration we measured the frequency shift according to Eq. (3.15). We have only taken into account the first two terms in Eq. (2.12) since higher orders contribute higher powers of α_0/σ_0^3 which is always a small quantity in practice. Taking the probability distribution of the frequency shifts we then obtained the line shape of the spectrum. Figure 1 presents the line shapes at different reduced densities of the solvent, while Fig. 2 shows the dependence of the line shapes on the impurity diameter. In particular, if the diameter of the impurity is smaller than that of the solvent particles, the width tends to increase rather rapidly. This may explain to a certain extent the broadening of the benzene line in argon at higher densities: Since benzene is a ring molecule the solvent particles can get very close to it and this effect could become significant when the density increases, leading to a decrease of the effective diameter with density.

TABLE I. The fitting of the predictions of the line shifts for benzene in other liquids (data in argon liquid is also presented for comparison); experimental data were taken from Refs. 10–12. The subscript E indicates "experiment" while the subscript S means "simulation." Presented in the last column are the expected values of the characteristic frequencies of the liquids appropriate for the theory.

Solvent	ω_0/ω_{0I}	σ_0	$\rho\sigma_0^3$	α_0	$[\Delta\omega_I]_E$	$[\Delta\omega_I]_S$	$\tilde{\omega}_0/\omega_0$
Ar	22	3.34 Å	0.50	1.64 Å^3	-60 cm^{-1}	-61 cm^{-1}	1.0
N_2	21.5	3.57 Å	0.80	1.76 Å^3	-140 cm^{-1}	-95 cm^{-1}	0.68
C_3H_8	7.6	4.7 Å	0.51	6.48 Å^3	-272 cm^{-1}	-147 cm^{-1}	0.54
He	34	2.33 Å	0.40	0.20 Å^3	30 cm^{-1}	-18 cm^{-1}	...

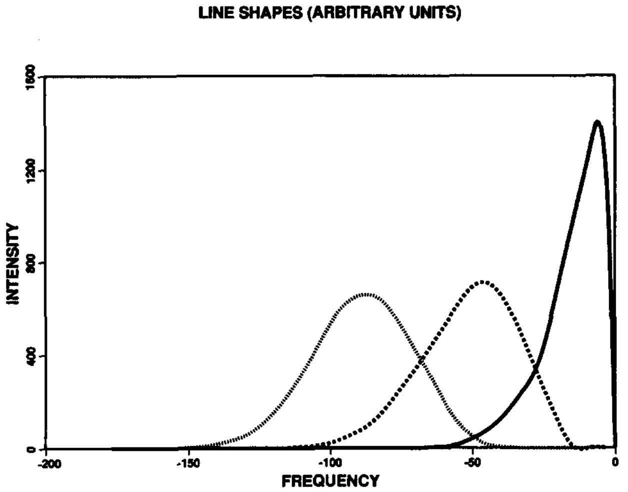

FIG. 1. The line shapes of the impurity spectrum with the hard core diameters of solute and solvent being equal, $\sigma_I = \sigma_0$. The simulations were conducted at the following reduced densities: $\rho\sigma_0^3 = 0.15$ (solid line), 0.45 (dashed line) and 0.70 (dotted line). The bare frequency of the impurity is located at the zero of the horizontal axis.

We now wish to compare the result of the computer simulations on the impurity line shift and linewidth with the experimental data for the benzene $^1B_{2u} \rightarrow {}^1A_{1g}$ transition in various liquids.[10–12] Let us first discuss the case of benzene in argon[12] since the structure of this solvent is relatively simple. We need to choose the following two parameters: the effective diameter of benzene and the characteristic frequency of the argon atom. The first quantity is rather vague in this context since the benzene molecule is highly nonspherical, while the second one should lie between the first excited state and the first ionization frequency of the solvent particle. The choice made in[12] is $\sigma_I = \sigma_0 = 3.34$ Å and $\hbar\omega_0 = 15.75$ eV. This first ionization energy of the argon atom, but the difference between this and the first excited-state energy is insignifiant (see below for the other cases). Using these choices, our fitting of the theoretical predictions to experiment is essentially parameter-free; it is presented in Fig. 3(a) and (b) for both the line shift and linewidth.The agreement between theory and experiment is very good, especially for the line shift in the low-density regime. There are discrepancies in the higher-density regime for the linewidth. This might be due to the nonspherical nature (there are some discussions in the literature to generalize the Drude model to include quadrupoles, see Refs. 16 and 25) of the solute or to the effects of the (exchange) repulsive interactions between the solute and solvent; the latter has not been considered in this theory (see discussions in Sec. 5).

We next discuss benzene in nitrogen and propane. We consider a typical value of the density in each case where the experimental data were presented numerically.[10,11] We shall continue to use the benezene diameter chosen above, in contrast to that in[10–12] where it was chosen to be the diameter of the new solvents. However, some care should be taken with regard to ω_0 since both the spectrum of the nitrogen and propane molecules are complicated—it is now questionable whether one can still take for ω_0 their first ionization frequencies. Table I presents the result using the first ionziation energy. This clearly underestimates the line shifts and we believe that the discrepancies are mainly due to the choice of ω_0. In the last column of the table, we present the modified

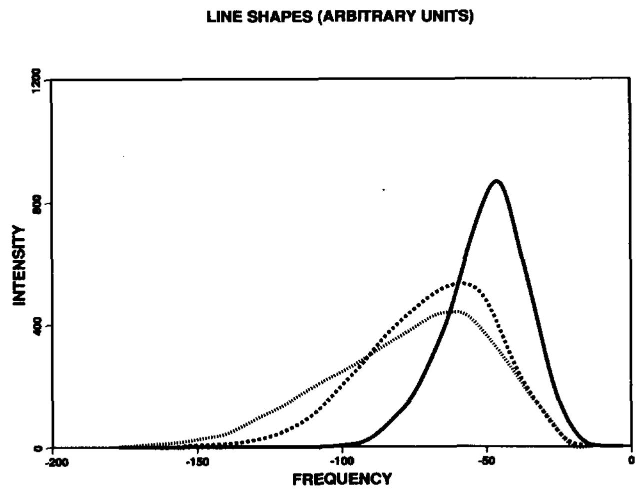

FIG. 2. The line shapes of the impurity spectrum (arbitrary units) at $\rho\sigma_0^3 = 0.5$ and $\sigma_I = 1.1\sigma_0$ (solid line), $0.9\,\sigma_0$ (dashed line) and $0.8\,\sigma_0$ (dotted line). The bare frequency of the impurity is located at the zero of the horizontal axis.

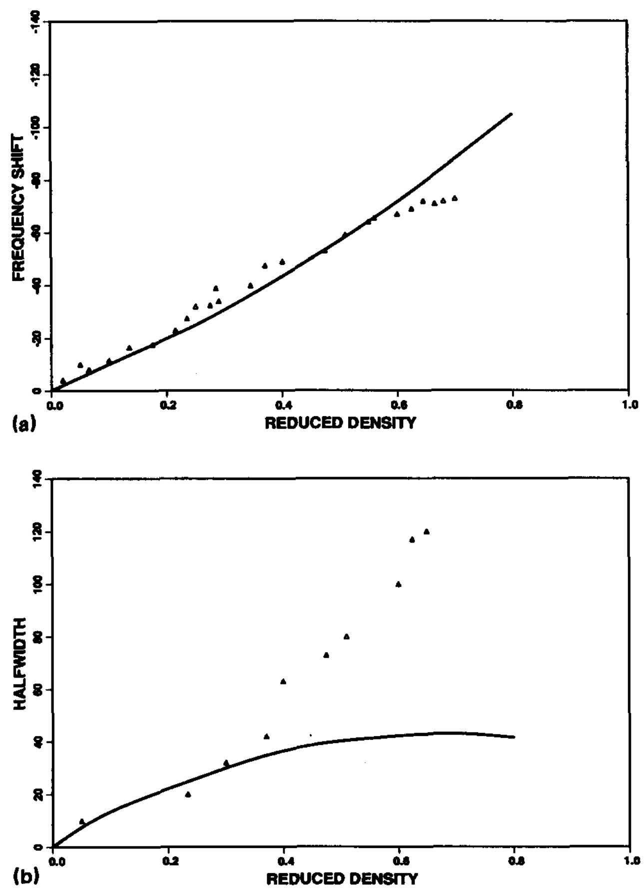

FIG. 3. Comparison of the Monte Carlo simulations with experiment: (a) The solid line is the prediction of the line shift of benzene $^1B_{2u} \rightarrow {}^1A_{1g}$ in argon liquid at room temperature; the experimental data were taken from Ref. 12. (b) The prediction (solid line) and the experimental data for the linewidth of the benzene spectrum in (a) where some unknown background broadening has been substrated.

characteristic frequencies $\tilde{\omega}_0$ which give the best fit: they are substantially smaller than the ionization frequencies. Further experimental information is required in order to carry out more accurate comparisons.

We also give, in the last row of Table I, the theoretical prediction for benzene in liquid helium. The predicted red shift is much smaller than those in the other cases discussed above. In fact, it was found experimentally[12] that the shift is mainly blue, indicating that the exchange repulsion between the benzene and helium atom may dominate the line shift. This effect is discussed in the next section.

V. DISCUSSIONS

A. Some remarks on the exchange repulsion

We now wish to consider the role of the exchange repulsion between different atoms. As seen in the last section, the theory based on dipolar interactions described here provides good predictions in the relatively low-density regime. As the density increases, the shift usually deviates from the theoretical predictions toward the blue side. In some cases, e.g., xeon in liquid argon,[13–15] the whole shift is mainly blue. There are various theories[13,14,16] explaining this blue shift as the result of the exchange repulsion between the atoms (see also Refs. 26 and 27). It would certainly be desirable to develop a model which takes into account the mechanisms for both types of shifts.

There are two important differences between the dipolar interaction and the exchange repulsion. First, the latter is rather static during the course of photon absorption since the positions of the atoms change slowly compared to their internal dynamics. Second, the influence of the exchange repulsion on the energy levels is rather direct: It gives first-order corrections to the energies of the ground and excited states and any difference between these corrections gives rise to a shift of the frequency.

Many of the existing theories[13,14,16] argue that the upper lever has a larger correction due primarily to the larger size of the atomic radius in the excited state so that it feels more repulsion from the surrounding atoms. Assuming that this picture is correct, let us introduce a typical difference δR between the hard core radii of the ground and excited states (see Ref. 13). Whenever a surrounding atom enters the excited state range of a given target atom it will induce a change in the excited state energy. Contributions from different "environmental particles" are additive. In our spin-boson model, we can add $\delta\Omega_0$ to Ω_0 (the frequency of the target atom):

$$\delta\Omega_0 = W \times \sum_{j>1} \theta(R_1 + \delta R + R_j - |\mathbf{r}_1 - \mathbf{r}_j|), \qquad (5.1)$$

where $\theta(x)$ is the usual step function, R_j is the radius of the atom j and W stands as a fitting parameter.

In general, the two effects can be considered separately to find the new line shift. On the other hand, to find the shape of the absorption spectrum, one has to find the joint fluctuations of both contributions to the shift—for this one has to rely on computer simulations. To fully explore the problem of the frquency dependent polarizability of a quantum liquid further investigations combining both of the effects, are certainly desirable.

B. Summary of results

We presented in this paper a new dynamical derivation of the frequency dependent polarizability obtained by Thompson, Schweizer, and Chandler[5] and by Høye and Stell.[6] Our derivation is based on the observation that for the Drude model the equations of motion describing the polarization of the atoms have the same form classically and quantum mechanically. Moreover, the Fourier transform of these equations shows the equivalence between the frequency independent and static polarizabilities. The existing results[1,3,4] for the latter case can therefore be utilized. Applying our approach to the case of impurity polarization we obtained both the line shift and the line shape of the impurity absorption spectrum.

We then considered the corrections due to the limited number of internal states involved. This was done by modeling the environment of a target atom by a bath of harmonic oscillators while taking into account details of the electronic properties of the target atom. Applying this to a two-level atom led to a prefactor ω_{0I}/ω_0 in the line shift computed by Chandler, Schweizer, and Wolynes.[9] In contrast, the resulting solvent polarizability remained the same in the small bandwidth limit. The prefactor greatly improves the agreement between theory and experiment for benzene in argon and some other liquids.[10–12] The line shape of the impurity spectrum was further calculated by Monte Carlo simulations. This gave qualitative agreement between theory and experiment. Finally, we discussed a simplified scheme to include both the effects of the exchange repulsion and dipole–dipole attraction forces.

ACKNOWLEDGMENTS

We wish to thank M. S. Wertheim and S. Baer for useful discussions and D. Chandler for valuable suggestions.

[1] M. S. Wertheim, Mol. Phys. **25**, 211 (1973).
[2] M. S. Wertheim, Mol. Phys. **26**, 1425 (1973); **33**, 95 (1977); and **34**, 1109 (1977).
[3] J. S. Høye and G. Stell, J. Chem. Phys. **72**, 1597 (1980); **73**, 461 (1980).
[4] L. R. Pratt, Mol. Phys. **40**, 347 (1980).
[5] J. S. Høye and G. Stell, J. Chem. Phys. **75**, 5133 (1981); J. S. Høye and K. Olaussen, *ibid.* **77**, 2583 (1982).
[6] M. J. Thompson, K. S. Schweizer, and D. Chandler, J. Chem. Phys. **76**, 1128 (1982).
[7] R. P. Feynman and A. R. Hibbs, *Quantum Mechanics and Path Intergrals* (McGraw–Hill, New York, 1965); R. P. Feynman, in *Statistical Mechanics* (Benjamin, Reading, MA, 1972), Chap. 3.
[8] D. Chandler and P. Wolynes, J. Chem. Phys. **74**, 4087 (1981).
[9] D. Chandler, K. S. Schweizer, and P. G. Wolynes, Phys. Rev. Lett. **49**, 1100 (1982); see also K. S. Schweizer and D. Chandler, J. Chem. Phys. **78**, 4118 (1983); K. S. Schweizer, *ibid.* **85**, 4638 (1986).
[10] R. Nowak and E. R. Bernstein, J. Chem. Phys. **86**, 3197 (1987).
[11] R. Nowak and E. R. Bernstein, J. Chem. Phys. **86**, 4783 (1987).
[12] R. Nowak and E. R. Bernstein, J. Chem. Phys. **87**, 2457 (1987).
[13] M. J. Saxton and J. M. Deutch, J. Chem. Phys. **60**, 2800 (1974).
[14] I. Messing, G. Raz, and Joshua Jortner, J. Chem. Phys. **66**, 2239 (1977).
[15] I. T. Steinberger and S. Baer, Phys. Rev. B **36**, 1358 (1987).
[16] V. Dobrosavljević, C. W. Henebry, and R. M. Stratt, J. Chem. Phys. **88**, 5781 (1988).
[17] S. Baer, Mol. Phys. **65**, 263 (1988).

[18] The case of photon emission needs more care since the life times of excited states are usually not so short compared to the motion of the positions so

that the atoms can adjust themselves if the radius of the excited states are significantly larger than that of the ground state (cf. Ref. 13 for more discussions). We shall ignore this for now.

[19]G. S. Rushbrooke, G. Stell, and J. S. Høye, Mol. Phys. **26**, 1199 (1973).
[20]M. S. Wertheim, J. Chem. Phys. **55**, 4291 (1971).
[21]S. Swain, J. Phys. A **5**, 1587 (1972).
[22]P. Pfeifer, Phys. Rev. A **26**, 701 (1982).
[23]R. W. Hall and P. G. Wolynes, J. Stat. Phys. **43**, 935 (1986).
[24]P. de Smedt, P. Nielaba, J. L. Lebowitz, and J. Talbot, Phys. Rev. A **38**, 1381 (1988).
[25]D. Logan, Mol. Phys. **51**, 1365, 1395 (1984).
[26]R. W. Hall and P. G. Wolynes, J. Chem. Phys. **83**, 3214 (1985).
[27]D. Logon and P. Edwards, Philos. Mag. B **53**, L23 (1986); B-C. Xu and R. M. Stratt, J. Chem. Phys. **89**, 7388 (1988).